Article type: Regular Manuscript

Seasonal and long-term consequences of esca on grapevine stem xylem integrity

G. Bortolami[a], E. Farolfi[a], E. Badel[b], R. Burlett[c], H. Cochard[b], N. Ferrer[a], A. King[d], L.J. Lamarque[c,e], P. Lecomte[a], M. Marchesseau-Marchal[a], J. Pouzoulet[f], J.M. Torres-Ruiz[b], S. Trueba[c,g], S. Delzon[c], G.A. Gambetta[f], C.E.L. Delmas[a*]

[a]INRAE, BSA, ISVV, SAVE, 33882 Villenave d'Ornon, France
[b]Université Clermont-Auvergne, INRAE, PIAF, 63000 Clermont-Ferrand, France
[c]Univ. Bordeaux, INRAE, BIOGECO, 33615 Pessac, France
[d]Synchrotron SOLEIL, L'Orme des Merisiers, Gif-sur-Yvette, 91192, France
[e]Département des Sciences de l'Environnement, Université du Québec à Trois-Rivières, Trois-Rivières, Québec, G9A 5H7, Canada
[f]EGFV, Bordeaux-Sciences Agro, INRAE, Université de Bordeaux, ISVV, 210 chemin de Leysotte, 33882 Villenave d'Ornon, France
[g]School of Forestry and Environmental Studies, Yale University, New Haven, CT 06511, USA

*Author for correspondence
Chloé E. L. DELMAS
Tel: +33557122636
Email: chloe.delmas@inrae.fr
ORCID ID: 0000-0003-3568-605X

SUMMARY

- Hydraulic failure has been extensively studied during drought-induced plant dieback, but its role in plant-pathogen interactions is under debate. During esca, a grapevine (*Vitis vinifera*) disease, symptomatic leaves are prone to irreversible hydraulic dysfunctions but little is known about the hydraulic integrity of perennial organs over the short- and long-term.
- We investigated the effects of esca on stem hydraulic integrity in naturally infected plants within a single season and across season(s). We coupled *in vivo* X-ray microtomography visualizations with direct (k_s) and indirect (k_{th}) hydraulic conductivity measurements, and tylose and vascular pathogen detection.
- Although no loss of hydraulic conductivity (PLC) was observed in asymptomatic and 40% of symptomatic stems, 60% of symptomatic stems presented xylem occlusions with subsequent PLC, which could reach critical levels (over 50% PLC). A loss of stem k_s was observed simultaneously, or after, the occurrence of leaf symptoms in the presence of tyloses. The impact of esca on xylem integrity was only seasonal and no long-term impact of disease history was recorded.
- Our study demonstrated how and to what extent a vascular disease such as esca, affecting xylem integrity, could amplify plant mortality by hydraulic failure.

Key words: Esca, hydraulic failure, plant dieback, vascular pathogens, *Vitis vinifera* L., tyloses, X-ray microCT, xylem anatomy

INTRODUCTION

In agricultural and forest ecosystems, perennial plant dieback causes decreases in plant productivity and longevity (Aleemullah & Walsh, 1996; Eskalen *et al*., 2013; Urbez-Torres *et al*., 2013; Alvindia & Gallema, 2017). Plant dieback is a complex process where different biotic and/or abiotic stress factors interact and contribute to leaf and crown wilting and ultimately plant death (Desprez-Lostau *et al*., 2006; Anderegg *et al*., 2013, Cailleret *et al*., 2017; Bettenfeld *et al*., 2020). Drought-mediated plant dieback has been extensively studied, and in this case hydraulic failure has been identified as the primary cause of plant death (Anderegg *et al*., 2016). Hydraulic failure results from an interruption of the ascendant water flow by air embolism or xylem occlusion (Zimmermann, 1983; Tyree & Sperry, 1989). Vascular pathogens, which infect the xylem network (Yadeta & Thomma, 2013), are also important drivers of pathogen-mediated plant dieback (Goberville *et al.*, 2016; Pandey *et al*., 2018; Fallon *et al*., 2020).

Vascular pathogens induce wood necrosis, leaf symptoms, and crown defoliation (Beckmann & Roberts, 1995; Pearce, 1996). Their biology and toxic metabolite production has been well studied, in particular using controlled phytotoxicity assays (Andolfi *et al.*, 2011; Akpaninyang & Opara, 2017). However, the possible role of hydraulic failure during pathogen-mediated plant dieback has been poorly investigated, and the underlying physiological mechanisms inducing leaf symptoms are not clear yet (Fradin & Thomma, 2006; McDowell *et al*., 2008). Moreover, the long-term impact (over seasons) and relationships between pathogens, leaf symptom presence, and the hydraulic functioning of the plant are still unknown. During vascular pathogenesis, both air (Pérez-Donoso *et al*., 2016) and non-gaseous (Sun *et al*., 2013; Pouzoulet *et al*., 2019) embolism have been observed. For example, air embolism is thought to accelerate pathogen progression during Pierce's disease (Pérez-Donoso *et al*., 2016), and non-gaseous embolism is associated with occlusion of the xylem conduits by the plant that could slow the disease process while interfering with xylem water transport (Sun *et al*., 2013; Pouzoulet *et al*., 2019).

Xylem occlusion, usually through the production of tyloses and gels, is one of the first plant defense mechanisms against vascular pathogens (Pearce, 1996). Xylem parenchyma cells secrete gels and expand into the vessel lumen, forming tyloses, physically blocking pathogen progression (Zimmermann, 1979). Xylem anatomy plays an important role, both for vascular pathogen development (Martin *et al*., 2009; Martín *et al*., 2013; Venturas *et al*., 2014;

Pouzoulet *et al*., 2017; 2020) and for tylose formation (Bonsen & Kucera, 1990; De Micco *et al*., 2016; Pouzoulet *et al*., 2019). If effective, this occlusion mechanism allows the plant to compartmentalize the infected zone and to generate new tissue around it (CODIT model, Pearce, 1996). Because tyloses can potentially interfere with the hydraulic functioning of the plant, they could exacerbate disease symptoms (Talboys, 1972). Tyloses are usually observed in close proximity to pathogens, as shown in artificial inoculation studies (Clerivet *et al,*. 2000; Rioux *et al*., 2018, among others). However, pathogens frequently proliferate in perennial organs without physically reaching the leaves, thus leaf symptoms are often induced at a distance (Beckmann & Roberts, 1995). A recent study shows that tyloses can be present in symptomatic leaves at a distance from the pathogen niches resulting in decreased leaf hydraulic conductivity (Bortolami *et al*., 2019).

Over the last decades, grapevine (*Vitis vinifera* L.) mortality and yield loss have been reported in European, American, and South African vineyards due to esca trunk disease (Cloete *et al*., 2015; Guerin-Dubrana *et al*., 2019). Esca affects mostly mature grapevines (more than seven-years-old), and symptoms include trunk necrosis and leaf symptoms, consisting of "tiger-stripe" necrosis and leaf wilting (Lecomte *et al*., 2012; Claverie *et al*., 2020), which are not regularly expressed season-to-season even within individual vines (Guerin-Dubrana *et al*., 2013; Li *et al*., 2017). While the pathogens responsible for esca-induced trunk necrosis have been identified (Morales-Cruz *et al*., 2018; Brown *et al*., 2020), the underlying mechanisms of leaf and fruit symptoms, and plant death are still poorly understood. Bortolami *et al*. (2019) demonstrated that the two vascular pathogens related to esca (*Phaeomoniella chlamydospora* and *Phaeoacremonium minimum*) were never detected in leaves or in one-year old stems, but always in the trunk (independently from leaf symptom presence). They further showed that esca symptomatic leaves presented significant losses in hydraulic conductivity due to the occlusion of the xylem conduits by tyloses. Together, these results suggest a relevant role of hydraulic failure in esca leaf symptom formation, but whether or not there is a corresponding failure in perennial organs, and the exact timing of these phenomena, are still unknown. As stems and branches are the direct connections between the pathogen niche in the trunk and the observed symptoms in the leaves, the study of stem xylem integrity is crucial in the understanding of leaf symptom formation in the current year and across seasons.

In this study, we investigated stem xylem integrity in grapevine during esca leaf symptom formation asking the following questions: (i) Can esca lead to hydraulic failure in perennial

111 organs? (ii) Does stem hydraulic failure occur prior to or after leaf symptom expression, and
112 does it depend on xylem anatomy? (iii) Do long-term symptomatic plants present different
113 xylem anatomy and levels of hydraulic failure from long-term asymptomatic plants? To answer
114 these questions, we transplanted 28-years-old grapevines (*Vitis vinifera* L. cv Sauvignon blanc)
115 from the field into pots to transport, manipulate, and study naturally esca-infected vines. We
116 coupled *in vivo* visualizations of stem xylem functionality (using synchrotron-based X-ray
117 microcomputed tomography) with stem specific hydraulic conductivity measurements (k_s),
118 theoretical hydraulic conductivity estimates (k_{th}), optical observations of vessel occlusions, and
119 pathogen detection during symptom appearance, while comparing plants with different
120 symptom history record.

121

122 # MATERIALS AND METHODS

123 ## Plant material

124 *Vitis vinifera* cv. Sauvignon blanc grafted onto 101-14 MGt were uprooted in winter 2017,
125 2018, and 2019 from a vineyard planted in 1992 located at INRAE Bordeaux-Nouvelle
126 Aquitaine (44°47'24.8"N, 0°34'35.1"W) and transferred into pots. Each of these plants has been
127 surveyed each year in the field since 2012 for esca leaf symptom expression following Lecomte
128 *et al*. (2012), and has been classified yearly as leaf-symptomatic or asymptomatic. Plants were
129 then classified by their long-term symptomatology record: plants asymptomatic from 2012 to
130 2018 (pA, previously asymptomatic), and plants that have expressed symptoms at least once
131 between 2012 and 2018 (pS, previously symptomatic). The uprooting method and greenhouse
132 growth conditions are detailed in Bortolami *et al*. (2019).

133 ## Esca symptom notation

134 The evolution of esca leaf symptoms was surveyed twice a week from June to October 2019
135 on every plant (n=84, Fig. 1). As presented in Fig. 1a, esca symptoms were scored at the stem
136 and whole plant scales. Single stems collected for analyses (both hydraulic measurements or
137 microCT observations) could be noted as: asymptomatic (green leaves and apparently healthy),
138 pre-symptomatic (leaves presenting yellowing or small yellow spots between the veins), tiger-
139 stripe (typical pattern of esca leaf symptoms), or apoplectic (leaves passing from green to
140 wilted in a couple of days). Along the experimentation, entire plants could be noted as

asymptomatic (control) or symptomatic (when at least 25% of the canopy was presenting tiger-stripe leaf symptoms). At the end of the experiment (week 40, October 2019) each plant was classified as symptomatic or asymptomatic (control). We were then able to group each stem measured into six different groups (Fig. 1a): one group of stems from control plants (asymptomatic from June to October) and five groups of stems from symptomatic plants: two before symptom appearance (asymptomatic and pre-symptomatic stems); and three after symptom appearance (asymptomatic, tiger-stripe, and apoplectic stems). To clearly differentiate asymptomatic stems collected from symptomatic plants and asymptomatic stems collected from asymptomatic plants, we considered plants (and their stems) that didn't show leaf symptoms during the experiment as control plants (or stems). We investigated whether symptom expression (final symptom notation in October 2019, see Fig. 1) differed between plants with contrasted long-term symptom history (previously asymptomatic vs previously symptomatic, Table 1) using a Chi-square test of independence.

X-ray microCT observation

Synchrotron-based microCT was used to visualize the content of vessels and their functionality in esca tiger-stripe and control stems. Three symptomatic plants (presenting tiger-stripe symptoms for 8, 7, and 3 weeks), and one asymptomatic-control plant were brought to the PSICHE beamline (King *et al.*, 2016) at SOLEIL synchrotron facility in September 2019. Shoots (ca. 2 m long) were cut under water and transferred into a solution containing 75mM of contrasting agent iohexol. The iohexol solution absorbs X-rays very strongly and appears bright white in X-ray scans above the iodine K-edge at 33.2 keV, and, once it has been taken up by the transpiration stream, the effective functionality of each vessel can be confirmed (Pratt & Jacobsen, 2018; Bortolami *et al.*, 2019). These stems were moved and left outdoor to transpire the solution for at least half a day. The stems were then transferred to the beamline stage and scanned twice in less than 5 minutes using two different energies of a high-flux (3×10^{11} photons mm^{-2}) monochromatic X-ray beam: 33.1 keV and 33.3 keV. The projections were recorded with a sCMOS camera equipped with a 250-mm-thick LuAG scintillator (Orca Flash, Hamamatsu, Japan). The complete tomographic scan included 1500 projections, and each projection lasted 50 ms. Tomographic reconstructions were performed using PyHST2 software (Mirone *et al.*, 2014) using the Paganin method (Paganin *et al.*, 2002), resulting in 32-bit

172 volume reconstructions of 2048 x 2048 x 1024 voxels. The final spatial resolution was 2.8769
173 μm^3 $voxel^{-1}$.

174 **Image analysis of microCT scans**

175 The contrast agent iohexol allowed us to distinguish in intact scans the effective functionality
176 of each vessel. In the absence of iohexol, X-ray microCT scans are used to distinguish air-filled
177 vessels (appearing black, corresponding to native PLC) from sap-filled vessels (appearing
178 grey). The addition of iohexol in the xylem sap allows to distinguish the functional vessels
179 (they appear bright white when they transport the sap), from the non-functional ones (i.e.
180 occluded vessels remaining grey, corresponding to occlusion PLC). We could also observe
181 partially occluded vessels (i.e. vessels with simultaneous presence of air and occlusions, or sap
182 and occlusions). This specific case was observed by checking the presence of any occlusion in
183 at least 200 slices in each volume. Partially occluded vessels were considered as occluded,
184 some examples are presented in Fig. S1. The equivalent-circle diameter of air-filled, occluded,
185 and functional (iohexol-filled) vessels was measured on the cross sections from the central slice
186 of the microCT scanned volume using ImageJ software (Schneider et al., 2012). Native PLC,
187 occlusion PLC, and total PLC (i.e. summing occlusion with native PLC) were calculated with
188 the Hagen-Poiseuille equation, as in Bortolami *et al*. 2019, (see Method S1). We investigated
189 whether native PLC, and occlusion PLC differed between control and esca tiger-stripe plants,
190 using two independent generalized mixed linear models where plants were treated as a random
191 effect. Proportional data (ranging from 0 to 1, dividing all PLC values by 100) was analyzed
192 to fit a logit link function and binomial distribution as appropriate.

193

194 **Monitoring stem hydraulic properties over time**

195 Stem xylem integrity was monitored over time by measuring hydraulic properties in control
196 and symptomatic plants along the season and during esca development. Stem specific hydraulic
197 conductivity (k_s) was measured by the gravity method (Sperry et al., 1988), and compared to
198 its theoretical analog (k_{th}) calculated from xylem anatomical observations on the same stem
199 (see below). When there are observed differences in k_s among stems, comparisons with
200 theoretical maximums (k_{th}) can show if lower k_s values result from anatomical differences (i.e.
201 different vessel size distributions) or by hydraulic failure (in the case of similar vessel size and
202 density). If k_s varies in unity with k_{th}, differences in k_s might result from anatomical differences

(e.g. smaller k_s are related to smaller vessels), otherwise k_s variations are the consequence of hydraulic failure. Each method to measure k_s, k_{th}, and to observe tyloses is described below.

Sampling started on June 19th and finished on September 13th 2019 for a total of 10 sampling dates, 39 stems from 23 control-asymptomatic plants, and 49 stems from 17 symptomatic plants. We randomly sampled control plants and esca symptomatic plants all along the season through the evolution of esca symptoms, obtaining measurements from 14 weeks before until 10 weeks after symptom appearance. To explore the contribution of the experimental design to data analysis, we tested the effect of the year of uprooting (2018 and 2019), the position of the analyzed internode, and the week of the measurement (i.e. evolution during the season) on k_s and k_{th} in control plants using separate generalized linear mixed model with normal distributions and the plant treated as a random variable (Table S1). A significant impact of the year of uproot was found for k_s and k_{th} values in control plants (Table S1). This could have resulted from the more favorable conditions (i.e. climatic stability and nutrient availability) for the greenhouse grown vines (note that plants uprooted in 2017 were only esca symptomatic and were not included in this analysis). However, once k_s and k_{th} are plotted together (Fig. S2), all the values lie on the same regression line without generating outlier values (smaller k_s values correspond to smaller k_{th} values independently of the uprooting year).

***Stem specific hydraulic conductivity* (k_s)**

k_s measurements were performed on one internode of >1.5m long one-year old stems, following Torres-Ruiz *et al*. (2012) gravity method (see Method S2 for details). A flow of 20 mM KCl solution passed through the sample from a reservoir to a precision electronic balance (AS220.R2, RADWAG, Radom, PL) recording the weight every 5 seconds using the WinWedge v3 5.0 software (TAL Technologies, Philadelphia, PA, USA). Hydraulic conductance, k [kg s^{-1} MPa^{-1}] was obtained by the slope generated by the flow and the corresponding pressure. The linear relationship between flow and pressure obtained were always characterized by R^2>0.97. Stem specific hydraulic conductivity, k_s [kg s^{-1} MPa^{-1} m^{-1}], was calculated as follows:

$$k_s = (k \times l) / A$$

$$A = ((d_1/2)^2 \times \pi) - ((d_2/2)^2 \times \pi)$$

Where: k is the hydraulic conductance, l is the length of the sample, A is the xylem area, d_1 is the external diameter of the debarked stem, and d_2 is the diameter of the central pith.

Stem theoretical hydraulic conductivity (k_{th}), vessel anatomy, and tylose observation

Just before hydraulic conductivity measurements, the lower internode was stored at 4 °C in 80% ethanol for analysis of xylem anatomy. When possible, the same internode of k_s measurements was used for anatomical analysis and k_{th} estimations, otherwise the stored internode was used for the following protocol. 50 µm thick slices were obtained using a GSL-1 microtome (Gärtner *et al.*, 2014). Slices were stained using a 0.5% safranin solution during 5 minutes, and then washed three to four times in ethanol (100%). They were quickly soaked in xylene and mounted on microscope slides with Permount Mounting Medium (Electron Microscopy Science, Hatfield, PA, USA). Images were captured with a stereo microscope SMZ1270 (Nikon, France) mounted with a DS-Fi3 camera (Nikon, France). The theoretical conductivity of each vessel (k_{vessel}) [kg m Mpa^{-1} s^{-1}] was calculated using the Hagen-Poiseuille equation:

$$k_{vessel} = (\pi \times \varnothing^4 \times \rho) / (128 \times \eta)$$

Where $\varnothing$ is the equivalent circle diameter [m] (measured with ImageJ software), ρ the density of water [998.2 kg m^{-3} at 20 °C], and η the viscosity of water [1.002 x 10^{-9} MPa s at 20 °C]. k_{th} of the stem [kg s^{-1} m^{-1} Mpa^{-1}] was then calculated by summing every k_{vessel} in the xylem area (A) [m²]:

$$k_{th} = \Sigma\, k_{vessel} / A$$

In the entire cross section of each sample, the physical presence (or absence) of tyloses in vessel lumina was visually assessed.

Regarding the statistical analysis, stems were grouped in six different categories following their esca symptomatology (as presented in Fig. 1a). We investigated whether k_s, k_{th}, and total vessel density differed among these different categories, and how k_s, k_{th}, and total vessel density differed between stems with and without tyloses (independently from leaf symptom presence), using independent mixed linear general models. The symptom / tylose category and the year of uprooting (since it had a significant impact on k_s and k_{th} in control plants, Table S1) were entered as fixed effects, with the plant treated as a random effect since different stems were

sometimes analyzed from the same plant (88 analyzed stems on 40 different plants). Total density and densities for each vessel diameter class were log-transformed prior to analysis to fit normality requirements. For the classes with no vessels (e.g. samples without vessel diameters above 160 µm), a minimal density of 0.0001 was assigned prior to log transformation. We investigated whether the frequency of symptomatic stems presenting tyloses changed with the symptom age (i.e. weeks between first symptom detection and k_s measurements on the same plant) with a Chi-square test. The relationships between stem k_s and k_{th} were tested using linear regression models. Finally, we investigated whether k_s and k_{th} in control stems differed between plants with different symptom history records using independent mixed linear general models with the plant treated as a random effect.

Fungal detection

Detection and quantification of *Phaeomoniella chlamydospora* and *Phaeoacremonium minimum* were performed using qPCR in a subsample of stems and trunks from the same symptomatic and control plants used for hydraulic and anatomical measurements. All along the season, basal internodes, from the same stems sampled for k_s and k_{th} measurements, were directly placed in liquid nitrogen and stored at -80 °C. At the end of the experiment, a subset of plants was cut at the base for trunk sampling. A 2 cm high section was cut with a sterilized hand saw. The bark was removed and the different tissues of each section (necrotic and apparently healthy wood) were separately collected using ethyl alcohol-sterilized shears in a sterile environment, and immediately placed in liquid nitrogen. All samples were ground in liquid nitrogen using a tissue lyser (Tissuelyser II, Qiagen, Germantown, MD, USA). DNA extraction and qPCR analysis were conducted as described in Pouzoulet *et al*. (2013) using the primer sets PchQF/R and PalQF/R. Detection and quantification of *P. chlamydospora* and *P. minimum* DNA by qPCR (SYBR Green assays) was conducted as described by Pouzoulet *et al*. (2017). After qPCR analysis, the results from each trunk sample (i.e. necrotic or apparently healthy wood) were averaged together in order to obtain one quantification per plant. Pathogen DNA quantity (average value of three technical replicates, fg/µl) was normalized by the amount of total DNA (ng/µl), detected using a Qubit fluorometer. We investigated whether the amount of fungal DNA (both for *P. chlamydospora* and for *P. minimum*) in trunks differed between symptomatic and control plants, and between control plants with different symptom history

292 records, using generalized linear mixed model with a poisson distribution and a log likelihood
293 function.

294

295 **Statistical analysis**

296 All data management and statistical tests were done in SAS software (SAS 9.4; SAS Institute).
297 We used PROC GLIMMIX for generalized linear mixed models, PROC GLM for generalized
298 linear models, PROC REG for regression analyses and PROC FREQ for frequency analyses
299 (Chi-square test of independence). The normality of the response variables was tested using a
300 Kolmogorov-Smirnov test (PROC UNIVARIATE) prior to analyses. Data were log-
301 transformed (total density) or appropriate distributions (binomial, poisson) were fitted when
302 appropriate.

303

304 # RESULTS

305 **Esca leaf symptom expression within and across seasons**

306 Esca leaf symptoms were recorded in 20 out of the 58 plants followed in this study (35%, Fig.
307 1, Table 1). The number of symptomatic plants increased gradually with time, from the first
308 symptom appearance in early June to the last in late September (Fig. 1). There was no effect of
309 the plant history (previously asymptomatic pA, or previously symptomatic pS) on 2019
310 symptom expression (n=58, X^2=0.27, P=0.60). On 20 pA plants, six (30%) expressed leaf
311 symptoms in 2019 (Table 1). On 38 pS plants, fourteen (37%) showed symptoms in 2019
312 (Table 1). However, pS plants expressed symptoms from June to the end of September, while
313 pA plants showed leaf symptoms only in September.

314

315 ***In vivo* observations of esca symptomatic stems**

316 Xylem vessels of control and tiger-stripe stems were observed using three dimensional X-ray
317 microCT scans in iohexol-fed samples (Fig. 2, 3, Table S2). As shown in Fig. 2, functional and
318 non-functional vessels can be discriminated through the use of iohexol (functional vessels
319 appear bright white, non functional vessels appear either black if air-filled or grey if occluded).

We observed almost totally functional stems in all asymptomatic stems (<20% total PLC, Fig. 2a-c), and 40% of tiger-stripe stems (e.g. Fig. 2d-g). Higher levels of PLC (>20% total PLC, Fig h-m) were observed in the remaining tiger-stripe stems, with 40% of tiger-stripe stems exhibiting over 50% total PLC (Fig. 2j-m). When the two components of PLC were disentangled, we observed that the level of native PLC remained low both in control (6.5 ± 2.6%) and in tiger-stripe (12.2 ± 2.9%) stems (Fig. 3a). Occlusion PLC values were virtually zero in control stems (0.7 ± 0.02%) while in tiger-stripe stems the mean occlusion PLC values was 27.5 ± 8.2% (Fig. 3b). Nevertheless, the variability of occlusion PLC across tiger-stripe stems was very high, the values ranging from 0.3% to 72.9% (Fig. 2d-m, and 3b), and occlusion PLC was not correlated to symptom age (n=10, $F_{2,7}$=0.19, P=0.83). Consequently, no statistical differences in native or occlusion PLC were found between control and tiger-stripe stems (Fig. 3). When higher occlusion PLC was measured (Fig. 2h-m), occluded vessels could be organized either on one side of the stem (Fig 2j-l) or randomly distributed across the section (Fig 2h, 2i, 2m). In 90% of symptomatic stems, we observed that the most external vessels were functional. Occlusions were present equally in all vessel diameter classes (Fig. S3).

Tylose development, stem specific (k_s) and theoretical (k_{th}) hydraulic conductivity during esca leaf symptom formation

Tyloses were identified in the xylem vessels of certain tiger-stripe stems and throughout the temporal development of esca leaf symptoms, from the appearance of symptoms to 11 weeks after. All apoplectic stems and 62.5% (15 of 24 analyzed stems) of esca tiger-stripe stems presented tyloses, while all other stems (control, asymptomatic or pre-symptomatic) did not contain these occlusions, even until one week before symptom development. In esca tiger-stripe stems, tyloses were not related to specific plants, or to symptom age (i.e. on the same plant at the same moment, different symptomatic stems could present tyloses, or not, n=24, X^2=7.47, P=0.38).

Overall, no significant impact of esca symptoms was observed on k_s (Fig. 4a), even if tiger-stripe stems were divided between those with and without tyloses. Control stems presented a mean (± SE) k_s of 24.97 ± 1.72 kg s^{-1} MPa^{-1} m^{-1}; all the stems without tyloses measured on symptomatic plants showed the same range of values as control stems (Fig 4a, Table 2): 26.04 ± 4.71 for asymptomatic before symptoms appearance, 30.32 ± 4.26 for pre-symptomatic

stems, 19.80 ± 5.18 for asymptomatic stems after symptom appearance on the plant, and 21.29 ± 5.40 for tiger-stripe stems without tyloses. Stems with tyloses (tiger-stripe and apoplectic stems) presented the lowest average k_s values (11.27 ± 2.86 and 2.47 ± 1.45 kg s^{-1} MPa^{-1} m^{-1} for tiger-stripe and apoplectic, respectively). Regarding k_{th}, no significant impact of esca symptoms was found (Fig. 4c, Table 2), all the values were in the same range, with average values ranging from 70.44 (for tiger-stripe stems with tyloses) to 87.88 (for pre-symptomatic stems) kg s^{-1} MPa^{-1} m^{-1}.

In order to further investigate the impact of esca on stem hydraulics, we explored the relationship between individual stem k_s and k_{th} in each symptom category (Fig. 4b, S4, Table 2). Significant relationships were found between k_s and k_{th} in all groups except in asymptomatic stems after symptom appearance and symptomatic stems with the physical presence of tyloses (Fig. S4, Table 2). The slopes of regression curves between k_s and k_{th} did not vary among groups in the absence of tyloses (slope values ranged between 0.3 and 0.4, Table 2) while it was close to 0 in the presence of tyloses (0.17 for tiger-stripe and 0.04 for apoplectic stems). When k_s and k_{th} are compared in the presence or absence of tyloses, we observed that k_s was significantly lower when tyloses were present (9.81 ± 2.51 kg s^{-1} MPa^{-1} m^{-1} in the presence of tyloses vs 25.06 ± 1.46 kg s^{-1} MPa^{-1} m^{-1} in the absence of tyloses, Table 2, n=88, $F_{1,49}$=7.11, P=0.01) while k_{th} did not significantly differ. Stems without tyloses presented a strong correlation between k_s and k_{th}, while in the presence of tyloses this relationship was not significant (Table 2, Fig. 4b).

Total vessel density did not significantly differ between stem symptomatology (comparing all the seven categories presented in Table 2), even when vessel density was partitioned by vessel diameter classes (Fig. 4d).

Finally, we tested the impact of disease history (comparing pA and pS plants) on the hydraulic conductivity and xylem anatomy in control plants. There were no differences between long-term symptomatic (pS) and long-term asymptomatic (pA) plants in stem k_s, stem k_{th}, or total vessel density (Table 3).

Fungal detection

The two vascular pathogens associated with esca (*Phaeomoniella chlamydospora* and *Phaeoacremonium minimum*) were never detected in one-year old stems while they were systematically detected in the trunk of both control and symptomatic plants (Table 4). In trunks, a significantly higher quantity of fungal DNA was detected in tiger-stripe symptomatic plants than in controls (Table 4). We found 2.14- and 1.64-fold more of *P. chlamydospora* and *P. minimum* DNA in symptomatic trunks relative to controls. In control plants, different symptom history record impacted the quantity of fungal DNA detected by qPCR, for *Phaeomoniella chlamydospora*, and for *Phaeoacremonium minimum*. We found 1.65- and 2.84-fold more *P. chlamydospora* and *P. minimum* DNA in previously symptomatic trunks relative to previously asymptomatic trunks (Table 3).

DISCUSSION

Our results regarding the xylem integrity during esca show that the presence of plant-derived tyloses induced hydraulic failure in 60% of symptomatic stems. Tyloses were produced simultaneously with, or after, the occurrence of leaf symptoms, and resulted in more than 50% PLC in 40% of symptomatic stems, unrelated to symptom age. We demonstrated that the presence of leaf symptoms during previous seasons had no impact on the likelihood of symptom appearance in the current year, or on stem hydraulic conductivity and xylem anatomy. Vascular fungi were never detected in the same organs as the tyloses (one-year old stems), and although they were present in trunks of both tiger-stripe and control plants, tiger-stripe plants showed higher quantities of fungal DNA. Among control plants that did not express symptoms in the year of the study, we found higher quantities of fungal DNA in those plants with a long-term history of symptom formation. As xylem occlusions were not present in the totality of tiger-stripe stems, they are unlikely to be the direct structural cause of esca leaf symptom. However, they could increase the risk of plant mortality, as they impair water transport in a majority of symptomatic stems.

In vivo xylem integrity observations and hydraulic vulnerability segmentation

Using direct X-ray microCT imaging in esca symptomatic stems, we found that hydraulic conductivity loss was almost entirely associated with the presence of tyloses. Different studies

have investigated the link between vascular pathogen development and hydraulic conductivity in stems (Collins *et al*., 2009; Lachenbruch & Zhao, 2019; Mensah *et al*., 2020). During biotic stresses, air embolisms have been shown to decrease hydraulic conductivity during bacterial leaf scorch disease (McElrone *et al*., 2003; 2008), Pierce's disease (Pérez-Donoso *et al*., 2016), and Pine wilt disease (Yazaki *et al*., 2018). In the case of fungal wilt diseases, the hydraulic conductivity loss was associated with non-gaseous embolism (i.e. tyloses) at the point of pathogen inoculation (Guerard *et al*., 2000; Sallé *et al*., 2008; Beier *et al*., 2017; Mensah *et al*., 2020), or with canker presence in naturally infected stems (Lachenbruch & Zhao, 2019).

Using iohexol we were able to visually observe the exact spatial organization of functional vessels. Interestingly, in some symptomatic samples we found functional vessels surrounding the non-functional xylem (Fig. 2j-l), suggesting that the plant was able to preserve the more external vessels from occlusions or to form new functional vessels after the loss of conductivity. Moreover, the sectoriality of the occlusions observed in Fig. 2j-l was reminiscent of the sectoriality observed in the distributions of trunk necrosis, especially on the brown stripe necrosis appearing along the vasculature (Lecomte *et al*., 2012).

Comparing these results with our precedent study using the same technique in leaves, we showed that esca symptomatic leaves presented higher levels of occlusion PLC (60.7 ± 6.80% in midribs, and 54.02 ± 8.72% in petioles, data from Bortolami *et al*., 2019) compared to stems (27.53 ± 8.24 %, occlusion PLC), suggesting hydraulic vulnerability segmentation (although PLC in leaves and stems were measured in different plants and years). The hydraulic segmentation theory relies on the fact that annual organs (i.e. leaves) are more vulnerable than perennial organs (i.e. stems) to drought induced air embolism (Tyree & Ewers, 1991). Grapevine is well known for exhibiting strong hydraulic vulnerability segmentation (Charrier *et al*., 2016; Hochberg *et al*., 2016; 2017). This is thought to be adaptive, where the higher vulnerability in leaves and petioles favors embolism formation and leaf shedding prior to embolism formation in stems, thus protecting the perennial organs. Our observations during esca pathogenesis demonstrate that, analogous to the hydraulic vulnerability segmentation theory, leaves appear more vulnerable to the formation of non-gaseous embolism as well, which could mitigate the risk of hydraulic failure in perennial organs. From another perspective, the difference may not be a direct effect of the specific organ's vulnerability to non-gaseous embolism, but a consequence of a difference in the accumulation of putative toxins and/or elicitors. Indeed, we confirmed here that esca leaf symptoms occur at a distance

from the pathogen niche because vascular pathogens were never detected in one-year old stems, suggesting that the plant may transport a signal (i.e. toxins or elicitors) from the infected trunk up to the leaves. If the signal accumulates in leaves in a higher amount than it does in the stems, and stimulates occlusion formation, stems would then be secondarily affected.

Hydraulic conductivity, tyloses, and vessel anatomy

Tyloses could have different impacts, both positive and negative, during wilt disease pathogenesis: (i) tyloses contribute to pathogen resistance as they aim to seal off vessel lumens and impede pathogens spread throughout the host (CODIT model, Pearce, 1996). This is the case regarding the susceptibility of different species or varieties to specific pathogens (Jacobi & MacDonald, 1980; Ouellette *et al*., 1999; Clerivet *et al.,* 2000; Et-Touil *et al*., 2005; Venturas *et al*., 2014; Park & Juzwik 2014; Rioux *et al*., 2018), in particular to *Phaeomoniella chlamydospora*, one of the pathogen associated with esca (Pouzoulet *et al*., 2017; 2020). (ii) In other studies, it has been shown that tyloses can exacerbate symptoms (Talboys, 1972): they cause a reduction in stem hydraulic conductivity, sometimes associated with a reduction in stomatal conductance in leaves and, in the most severe cases, wilting (Parke *et al*., 2007; Beier *et al*., 2017; Lachenbruch & Zhao, 2019, Mensah *et al*., 2020 during fungi development; Sun *et al*., 2013; Deyett *et al*., 2019 during Pierce's disease). Our results suggest that during esca (i) the development of tyloses in stems cannot be interpreted as a systematic trait of pathogen resistance because visual symptoms were observed despite the presence of tyloses and they were produced at a distance from pathogens. (ii) When present, tyloses might lead to symptom exacerbation. Esca has also been suggested to lead to a general reduction in xylem water transport and stomatal conductance (Ouadi *et al*., 2019), and tyloses could be a major contributor to these phenomena as during winter senescence (Salleo *et al*., 2002; Sun *et al*., 2008). However, when stems have no tyloses, esca leaf symptom formation seems to arise from within the leaf itself, and does not result from upstream hydraulic failure.

Xylem is the battleground between vascular pathogens and the plant's defense response (Yadeta & Thomma, 2013). Even if xylem vessel anatomy is less investigated, it could have a crucial role in plant resistance and response to vascular pathogens. For example, during Dutch elm wilt disease (due to *Ophiostoma spp.*) the most sensitive species and varieties present wider xylem vessels (Elgersma, 1970; Mcnabb *et al*., 1970; Solla & Gil 2002; Pita *et al*., 2018).

Smaller vessels could occlude faster, sustaining a more efficient pathogen restriction (Venturas *et al*., 2014). Our results on xylem vessel anatomy suggest that stems with tyloses tend to present higher densities of small vessels, even if we did not observe any differences in total k_{th} values. Moreover, microCT scans showed that occlusions appear randomly in every vessel size class (Fig. S3). In contrast, artificial inoculations showed that xylem vessel diameter had a strong impact on esca-related vascular pathogen development (Pouzoulet *et al*., 2017; 2020), and in the kinetic of vessel occlusion in grapevine stems (Pouzoulet *et al*., 2019). The relationships between esca leaf symptoms, xylem anatomy, and tylose presence should be studied in detail in trunks, where vascular pathogens are present, and among different grapevine varieties and rootstocks as they are known to show different susceptibility to symptom expression.

Long-term consequences of esca on leaf symptom expression and stem hydraulic integrity

In field surveys, esca leaf symptoms are often randomly distributed spatially throughout vineyards and are not consistent from season to season in individual vines (Mugnai *et al*., 1999; Surico *et al*., 2000; Marchi *et al*., 2006; Guerin-Dubrana *et al*., 2013; Li *et al*., 2017). However, esca-related vine death is strongly related to leaf symptoms as death is usually observed following a year with symptom expression (Guerin-Dubrana *et al*., 2013). In agreement with these field studies, we observed similar percentages of symptomatic plants between those that had already expressed esca symptoms in the past (from one to seven consecutive years, pS plants), and those that had never expressed symptoms over the past seven years (pA plants). However, we also found that pS plants expressed symptoms earlier in the season than pA plants, suggesting that symptoms might require more time to develop in pA plants. We did not find any significant differences in k_s and k_{th} values between plants with contrasted long-term symptom history. This result suggests that esca leaf symptoms may have xylem anatomical consequences within the year of expression by the production of tyloses, but not across seasons. Moreover, we showed that DNA pathogen amount (*Phaeoacremonium minimum* and *Phaeomoniella chlamydospora*) depends on the symptom expression in the season of sampling, and on the long-term symptom history. Altogether, these results suggest that a higher amount of vascular fungi in the trunk represents a higher risk in reproducing leaf symptoms, and consequently, a higher risk of plant death.

Hydraulic failure and esca leaf symptom pathogenesis

Our results showed that, even if esca-related stem occlusion was extremely variable, 40% of the microCT analyzed stems presented a total PLC greater than 50%. Under drought conditions alone, studies suggest that grapevines are not able to recover in the current season from PLC greater than 50% in stems (Charrier *et al*., 2018). Thus, to what extent these levels of esca-induced hydraulic failure compromise future vine performance, and/or increase the likelihood of developing esca leaf symptoms in the future remains an open question.

We showed that, similarly to visual leaf symptoms, tyloses in stems were generated at a distance from the pathogen niche in the trunk. Comparing our results with Bortolami *et al.* (2019), we show that hydraulic failure affected leaves, on average, two times more than stems. We could hypothesize that, following pathogen activities in the trunk, a signal passing through the xylem network and stimulating tyloses, first accumulates in leaves and then affects the stems. However, the exact signal and action remain unknown, as we showed that the presence of tyloses depended upon given symptomatic stems rather than symptomatic plants (i.e. two stems in the same plant, with same tiger-stripe symptoms, sampled at the same moment, could or could not present tyloses).

We showed that there were no differences in symptom expression, nor in the stem hydraulic properties, regarding the long-term symptom history. We can conclude that the processes that generate tiger-stripe symptoms are largely restricted to the current year of the symptom expression. However, in plants expressing symptoms for the first time according to our disease record, these processes could require more time, as they showed symptoms only late in the season. The presence of occlusion, leading to hydraulic failure in stems, could exacerbate leaf symptom expression in the following seasons, possibly contributing to death. We could speculate that a stem expressing extensive hydraulic failure could be more prone to express symptoms in the following year or, in the worst cases, to die. If the level of hydraulic failure could affect the stem mortality in the following year, the choice of stems with a complete absence of failure during the winter pruning could reduce the impact of esca in vineyards. In addition, the presence of occlusions could also amplify plant susceptibility to drought-induced hydraulic failure, enhancing the risk of plant mortality in the field as suggested by McDowell et al. (2008). It could be speculated that a decrease in soil water potential or a high evaporative

demand, concomitant to esca-induced hydraulic failure, could embolize the remaining functional xylem vessels stopping the water flow and desiccating plant tissues (this could be the case in apoplectic plants for example). In perspective, future studies should investigate the link between pathogen activities and occlusion development, especially in trunks, and the subsequent hydraulic failure consequences on whole plant physiology.

ACKNOWLEDGMENTS

We thank the experimental teams of UMR SAVE and UMR EGFV (Bord'O platform, INRAE, Bordeaux, France) and the SOLEIL synchrotron facility (beamline PSICHE) for providing the materials and logistics. Specifically, we thank Jérôme Jolivet and Sebastien Gambier (UMR SAVE) for providing technical knowledge and support for plant transplantation and maintenance. This work was supported by the French Ministry of Agriculture, Agrifood, and Forestry (FranceAgriMer and CNIV) within the PHYSIOPATH project (program Plan National Dépérissement du Vignoble, 22001150-1506) awarded to C.E.L.D., and program Investments for the Future (ANR-10-EQPX-16, XYLOFOREST).

Author contributions

C.E.L.D., G.A.G., G.B., and S.D. designed the experiments;

E.F., G.A.G., S.D., E.B., R.B., H.C., A.K., L.J.L., J.M.T.-R., S.T. participated in synchrotron campaigns;

G.B., C.E.L.D., E.F., and N.F. conducted the esca symptom notations;

G.B., M.M.-M.,and N.F. conducted the histological observations;

E.F. conducted the hydraulic conductivity measurements and participated to data analyses;

N.F., and J.P., conducted the pathogen detection;

G.B. analyzed the microCT, optical images, and analyzed the data;

P.L. provided data on disease history of the plants;

G.B., C.E.L.D., and G.A.G. wrote the article;

all authors edited and agreed on the last version of the article.

Data Availability Statement

We agree to archive the data associated with this manuscript should the manuscript be accepted.

REFERENCES

Akpaninyang, F. E., & Opara, E. U. (2017). The Influence of Toxins in Disease Symptom Initiation in Plants : A Review. *Journal of Agriculture and Sustainability*, *10*(1), 29-52.

Aleemullah, M., & Walsh, K. (1996). Australian papaya dieback : Evidence against the calcium deficiency hypothesis and observations on the significance of laticifer autofluorescence. *Australian Journal of Agricultural Research*, *47*(3), 371-385. https://doi.org/10.1071/AR9960371

Alvindia, D. G., & Gallema, F. L. M. (2017). *Lasiodiplodia theobromae* causes vascular streak dieback (VSD)–like symptoms of cacao in Davao Region, Philippines. *Australasian Plant Disease Notes*, *12*(1). https://doi.org/10.1007/s13314-017-0279-9

Anderegg, W. R. L., Kane, J. M., & Anderegg, L. D. L. (2013). Consequences of widespread tree mortality triggered by drought and temperature stress. *Nature Climate Change*, *3*(1), 30-36. https://doi.org/10.1038/nclimate1635

Anderegg, W. R. L., Klein, T., Bartlett, M., Sack, L., Pellegrini, A. F. A., Choat, B., & Jansen, S. (2016). Meta-analysis reveals that hydraulic traits explain cross-species patterns of drought-induced tree mortality across the globe. *Proceedings of the National Academy of Sciences*, *113*(18), 5024-5029. https://doi.org/10.1073/pnas.1525678113

Andolfi, A., Mugnai, L., Luque, J., Surico, G., Cimmino, A., & Evidente, A. (2011). Phytotoxins Produced by Fungi Associated with Grapevine Trunk Diseases. *Toxins*, *3*(12), 1569-1605. https://doi.org/10.3390/toxins3121569

Beckman, C. H., & Roberts, E. M. (1995). On the Nature and Genetic Basis for Resistance and Tolerance to Fungal Wilt Diseases of Plants. In *Advances in Botanical Research* 21, 35-77. Elsevier. https://doi.org/10.1016/S0065-2296(08)60008-7

Beier, G. L., Held, B. W., Giblin, C. P., Cavender-Bares, J., & Blanchette, R. A. (2017). American elm cultivars : Variation in compartmentalization of infection by *Ophiostoma novo-ulmi* and its effects on hydraulic conductivity. *Forest Pathology*, *47*(6), 1-11. https://doi.org/10.1111/efp.12369

Bettenfeld, P., Fontaine, F., Trouvelot, S., Fernandez, O., & Courty, P.-E. (2020). Woody Plant Declines. What's Wrong with the Microbiome? *Trends in Plant Science*, *25*(4), 381-394. https://doi.org/10.1016/j.tplants.2019.12.024

Bonsen, K. J. M., & Kučera, L. J. (1990). Vessel Occlusions in Plants : Morphological, Functional and Evolutionary Aspects. *IAWA Journal*, *11*(4), 393-399. https://doi.org/10.1163/22941932-90000528

Bortolami, G., Gambetta, G. A., Delzon, S., Lamarque, L. J., Pouzoulet, J., Badel, E., Burlett, R., Charrier, G., Cochard, H., Dayer, S. et al. (2019). Exploring the Hydraulic Failure Hypothesis of Esca Leaf Symptom Formation. *Plant Physiology*, *181*(3), 1163-1174. https://doi.org/10.1104/pp.19.00591

Brown, A. A., Lawrence, D. P., & Baumgartner, K. (2020). Role of basidiomycete fungi in the grapevine trunk disease esca. *Plant Pathology*, *69*(2), 205-220. https://doi.org/10.1111/ppa.13116

Cailleret, M., Jansen, S., Robert, E. M. R., Desoto, L., Aakala, T., Antos, J. A., Beikircher, B., Bigler, C., Bugmann, H., Caccianiga, M., et al. (2017). A synthesis of radial growth patterns preceding tree mortality. *Global Change Biology*, *23*(4), 1675-1690. https://doi.org/10.1111/gcb.13535

Charrier, G., Delzon, S., Domec, J.-C., Zhang, L., Delmas, C. E. L., Merlin, I., Corso, D., King, A., Ojeda, H., Ollat, N., et al. (2018). Drought will not leave your glass empty: Low risk of hydraulic failure revealed by long-term drought observations in world's top wine regions. *Science Advances*, *4*(1), 1-9 https://doi.org/10.1126/sciadv.aao6969

Charrier, G., Torres-Ruiz, J. M., Badel, E., Burlett, R., Choat, B., Cochard, H., Delmas, C. E. L., Domec, J.-C., Jansen, S., King, A., et al. (2016). Evidence for Hydraulic Vulnerability Segmentation and Lack of Xylem Refilling under Tension. *Plant Physiology*, *172*(3), 1657-1668. https://doi.org/10.1104/pp.16.01079

Claverie, M., Notaro, M., Fontaine, F., & Wery, J. (2020). Current knowledge on Grapevine Trunk Diseases with complex etiology : A systemic approach. *Phytopathologia Mediterranea*, *59*, 29-53. https://doi.org/10.14601/Phyto-11150

622 Clérivet, A., Déon, V., Alami, I., Lopez, F., Geiger, J.-P., & Nicole, M. (2000). Tyloses and
623 gels associated with cellulose accumulation in vessels are responses of plane tree seedlings
624 (*Platanus* × *acerifolia*) to the vascular fungus *Ceratocystis fimbriata* f. Sp *platani*. *Trees*, *15*(1),
625 25-31. https://doi.org/10.1007/s004680000063

626 Cloete, M., Mostert, L., Fischer, M., & Halleen, F. (2015). Pathogenicity of South African
627 Hymenochaetales taxa isolated from esca-infected grapevines. *Phytopathologia Mediterranea*,
628 *54*(2), 368-379. https://doi.org/10.14601/Phytopathol_Mediterr-16237

629 Collins, B. R., Parke, J. L., Lachenbruch, B., & Hansen, E. M. (2009). The effects of
630 Phytophthora ramorum infection on hydraulic conductivity and tylosis formation in tanoak
631 sapwood. *Canadian Journal of Forest Research*, *39*(9), 1766-1776.
632 https://doi.org/10.1139/X09-097

633 Desprez-Loustau, M.-L., Marçais, B., Nageleisen, L.-M., Piou, D., & Vannini, A. (2006).
634 Interactive effects of drought and pathogens in forest trees. *Annals of Forest Science*, *63*(6),
635 597-612. https://doi.org/10.1051/forest:2006040

636 Deyett, E., Pouzoulet, J., Yang, J. -I., Ashworth, V. E., Castro, C., Roper, M. C., & Rolshausen,
637 P. E. (2019). Assessment of Pierce's disease susceptibility in *Vitis vinifera* cultivars with
638 different pedigrees. *Plant Pathology*, *68*(6), 1079-1087. https://doi.org/10.1111/ppa.13027

639 De Micco, V., Balzano, A., Wheeler, E. A., & Baas, P. (2016). Tyloses and gums : A review
640 of structure, function and occurrence of vessel occlusions. *IAWA Journal*, *37*(2), 186-205.
641 https://doi.org/10.1163/22941932-20160130

642 Elgersma, D. M. (1970). Length and diameter of xylem vessels as factors in resistance of elms
643 to Ceratocystis ulmi. *Netherlands Journal of Plant Pathology*, *76*(3), 179-182.
644 https://doi.org/10.1007/BF01974328

645 Eskalen, A., Stouthamer, R., Lynch, S. C., Rugman-Jones, P. F., Twizeyimana, M., Gonzalez,
646 A., & Thibault, T. (2013). Host Range of Fusarium Dieback and Its Ambrosia Beetle
647 (Coleoptera : Scolytinae) Vector in Southern California. *Plant Disease*, *97*(7), 938-951.
648 https://doi.org/10.1094/PDIS-11-12-1026-RE

649 Et-Touil, A., Rioux, D., Mathieu, F. M., & Bernier, L. (2005). External symptoms and
650 histopathological changes following inoculation of elms putatively resistant to Dutch elm

disease with genetically close strains of *Ophiostoma*. *Canadian Journal of Botany*, *83*, 656–667.

Fallon, B., Yang, A., Lapadat, C., Armour, I., Juzwik, J., Montgomery, R. A., & Cavender-Bares, J. (2020). Spectral differentiation of oak wilt from foliar fungal disease and drought is correlated with physiological changes. *Tree Physiology*, *40*(3), 377-390. https://doi.org/10.1093/treephys/tpaa005

Fradin, E. F., & Thomma, B. P. H. J. (2006). Physiology and molecular aspects of *Verticillium* wilt diseases caused by *V. dahliae* and *V. albo-atrum*. *Molecular Plant Pathology*, *7*(2), 71-86. https://doi.org/10.1111/j.1364-3703.2006.00323.x

Gärtner, H., Lucchinetti, S., & Schweingruber, F. H. (2014). New perspectives for wood anatomical analysis in dendrosciences: the GSL1-microtome. *Dendrochronologia*, *32*(1), 47-51. https://doi.org/10.1016/j.dendro.2013.07.002

Goberville, E., Hautekèete, N.-C., Kirby, R. R., Piquot, Y., Luczak, C., & Beaugrand, G. (2016). Climate change and the ash dieback crisis. *Scientific Reports*, *6*(1). https://doi.org/10.1038/srep35303

Guérard, N., Maillard, P., Bréchet, C., Lieutier, F., & Dreyer, E. (2007). Do trees use reserve or newly assimilated carbon for their defense reactions? A 13C labeling approach with young Scots pines inoculated with a bark-beetle-associated fungus (*Ophiostoma brunneo ciliatum*). *Annals of Forest Science*, *64*(6), 601-608. https://doi.org/10.1051/forest:2007038

Guerin-Dubrana, L., Labenne, A., Labrousse, J. C., Bastien, S., Rey, P., & Gegout-Petit, A. (2013). Statistical analysis of grapevine mortality associated with esca or Eutypa dieback foliar expression. *Phytopathologia Mediterranea*, *52*(2), 276-288.

Guerin-Dubrana, L., Fontaine, F., & Mugnai, L. (2019). Grapevine trunk disease in European and Mediterranean vineyards : Occurrence, distribution and associated disease-affecting cultural factors. *Phytopathologia Mediterranea*, *58*(1), 49-71. https://doi.org/10.14601/Phytopathol_Mediterr-25153

Hochberg, U., Albuquerque, C., Rachmilevitch, S., Cochard, H., David-Schwartz, R., Brodersen, C. R., McElrone, A., & Windt, C. W. (2016). Grapevine petioles are more sensitive to drought induced embolism than stems : Evidence from *in vivo* MRI and microcomputed

680 tomography observations of hydraulic vulnerability segmentation: Hydraulic vulnerability
681 segmentation in grapevine. *Plant, Cell & Environment*, *39*(9), 1886-1894.
682 https://doi.org/10.1111/pce.12688

683 Hochberg, U., Windt, C. W., Ponomarenko, A., Zhang, Y.-J., Gersony, J., Rockwell, F. E., &
684 Holbrook, N. M. (2017). Stomatal Closure, Basal Leaf Embolism, and Shedding Protect the
685 Hydraulic Integrity of Grape Stems. *Plant Physiology*, *174*(2), 764-775.
686 https://doi.org/10.1104/pp.16.01816

687 Jacobi, W. R., & MacDonald, W. L. (1980). Colonization of resistant and susceptible oaks by
688 Ceratocystis fagacearum. *Phytopathology*, *70*(7), 618-623.

689 King, A., Guignot, N., Zerbino, P., Boulard, E., Desjardins, K., Bordessoule, M., Leclerq, N.,
690 Le, S., Renaud, G., Cerato, M., Bornert, M., et al. (2016). Tomography and imaging at the
691 PSICHE beam line of the SOLEIL synchrotron. *Review of Scientific Instruments*, *87*(9),
692 093704. https://doi.org/10.1063/1.4961365

693 Lachenbruch, B., & Zhao, J.-P. (2019). Effects of phloem on canopy dieback, tested with
694 manipulations and a canker pathogen in the Corylus avellana/Anisogramma anomala
695 host/pathogen system. *Tree Physiology*, *39*(7), 1086-1098.
696 https://doi.org/10.1093/treephys/tpz027

697 Lecomte, P., Darrieutort, G., Liminana, J.-M., Comont, G., Muruamendiaraz, A., Legorburu,
698 F.-J., Choueiri, E., Jreijiri, F., El Amil, R., & Fermaud, M. (2012). New Insights into Esca of
699 Grapevine : The Development of Foliar Symptoms and Their Association with Xylem
700 Discoloration. *Plant Disease*, *96*(7), 924-934. https://doi.org/10.1094/PDIS-09-11-0776-RE

701 Li, S., Bonneu, F., Chadoeuf, J., Picart, D., Gégout-Petit, A., & Guérin-Dubrana, L. (2017).
702 Spatial and Temporal Pattern Analyses of Esca Grapevine Disease in Vineyards in France.
703 *Phytopathology*, *107*(1), 59-69. https://doi.org/10.1094/PHYTO-07-15-0154-R

704 Martin, N., Vesentini, D., Rego, C., Monteiro, S., Oliveira, H., & Ferreira, R. B. (2009).
705 *Phaeomoniella chlamydospora* infection induces changes in phenolic compounds content in
706 *Vitis vinifera*. *Phytopathologia Mediterranea*, *48*(1), 101-116.
707 http://dx.doi.org/10.14601/Phytopathol_Mediterr-2879

708 Martín, J. A., Solla, A., Ruiz-Villar, M., & Gil, L. (2013). Vessel length and conductivity of
709 Ulmus branches : Ontogenetic changes and relation to resistance to Dutch elm disease. *Trees*,
710 *27*(5), 1239-1248. https://doi.org/10.1007/s00468-013-0872-2

711 McDowell, N., Pockman, W. T., Allen, C. D., Breshears, D. D., Cobb, N., Kolb, T., Plaut, J.,
712 Sperry, J., West, A., Williams, D. G., & Yepez, E. A. (2008). Mechanisms of plant survival
713 and mortality during drought : Why do some plants survive while others succumb to drought?
714 *New Phytologist*, *178*(4), 719-739. https://doi.org/10.1111/j.1469-8137.2008.02436.x

715 McElrone, A. J., Sherald, J. L., & Forseth, I. N. (2003). Interactive effects of water stress and
716 xylem-limited bacterial infection on the water relations of a host vine. *Journal of Experimental*
717 *Botany*, *54*(381), 419-430. https://doi.org/10.1093/jxb/erg046

718 McElrone, A. J., Jackson, S., & Habdas, P. (2008). Hydraulic disruption and passive migration
719 by a bacterial pathogen in oak tree xylem. *Journal of Experimental Botany*, *59*(10), 2649-2657.
720 https://doi.org/10.1093/jxb/ern124

721 McNabb, H. S., Heybroek, H. M., & Macdonald, W. L. (1970). Anatomical factors in resistance
722 to Dutch elm disease. *Netherlands Journal of Plant Pathology*, *76*(3), 196-205.
723 https://doi.org/10.1007/BF01974331

724 Mensah, J. K., Sayer, M. A. S., Nadel, R. L., Matusick, G., & Eckhardt, L. G. (2020).
725 Physiological response of *Pinus taeda* L. trees to stem inoculation with *Leptographium*
726 *terebrantis*. *Trees*. https://doi.org/10.1007/s00468-020-01965-0

727 Mirone, A., Brun, E., Gouillart, E., Tafforeau, P., & Kieffer, J. (2014). The PyHST2 hybrid
728 distributed code for high speed tomographic reconstruction with iterative reconstruction and a
729 priori knowledge capabilities. *Nuclear Instruments and Methods in Physics Research Section*
730 *B: Beam Interactions with Materials and Atoms*, *324*, 41-48.
731 https://doi.org/10.1016/j.nimb.2013.09.030

732 Morales-Cruz, A., Allenbeck, G., Figueroa-Balderas, R., Ashworth, V. E., Lawrence, D. P.,
733 Travadon, R., Smith, R. J., Baumgartner, K., Rolshausen, P. E., & Cantu, D. (2018). Closed-
734 reference metatranscriptomics enables *in planta* profiling of putative virulence activities in the
735 grapevine trunk disease complex : Transcriptomics of pathogen communities. *Molecular Plant*
736 *Pathology*, *19*(2), 490-503. https://doi.org/10.1111/mpp.12544

737 Mugnai, L., Graniti, A., & Surico, G. (1999). Esca (Black Measles) and Brown Wood-
738 Streaking : Two Old and Elusive Diseases of Grapevines. *Plant Disease*, *83*(5), 404-418.
739 https://doi.org/10.1094/PDIS.1999.83.5.404

740 Ouadi, L., Bruez, E., Bastien, S., Vallance, J., Lecomte, P., Domec, J.-C., & Rey, P. (2019).
741 Ecophysiological impacts of Esca, a devastating grapevine trunk disease, on *Vitis vinifera* L.
742 *PLOS ONE*, *14*(9), 1-20. https://doi.org/10.1371/journal.pone.0222586

743 Ouellette, G. B., Baayen, R. P., Simard, M., & Rioux, D. (1999). Ultrastructural and
744 cytochemical study of colonization of xylem vessel elements of susceptible and resistant
745 Dianthus caryophyllus by Fusarium oxysporum f.sp. Dianthi. *Can. J. Bot.*, *77*, 644-663.

746 Paganin, D., Mayo, S. C., Gureyev, T. E., Miller, P. R., & Wilkins, S. W. (2002). Simultaneous
747 phase and amplitude extraction from a single defocused image of a homogeneous object.
748 *Journal of Microscopy*, *206*(1), 33-40. https://doi.org/10.1046/j.1365-2818.2002.01010.x

749 Pandey, S., Rishi, R. R., Jayaraj, R., Giri, K., Kumar, R., Pandey, A., Juwantha, R., Madaan,
750 S., & Bhandari, M. S. (2019). *Fusarium equiseti* is associated with the wilt and dieback of
751 *Aquilaria malaccensis* in Northeast India. *Forest Pathology*, *49*(2), e12489.
752 https://doi.org/10.1111/efp.12489

753 Park, J.-H., & Juzwik, J. (2014). *Ceratocystis smalleyi* colonization of bitternut hickory and
754 host responses in the xylem. *Forest Pathology*, *44*(4), 282-292.
755 https://doi.org/10.1111/efp.12098

756 Parke, J. L., Oh, E., Voelker, S., Hansen, E. M., Buckles, G., & Lachenbruch, B. (2007).
757 *Phytophthora ramorum* Colonizes Tanoak Xylem and Is Associated with Reduced Stem Water
758 Transport. *Phytopathology*, *97*(12), 1558-1567. https://doi.org/10.1094/PHYTO-97-12-1558

759 Pearce, R. B. (1996). Antimicrobial defences in the wood of living trees. *New Phytologist*,
760 *132*(2), 203-233. https://doi.org/10.1111/j.1469-8137.1996.tb01842.x

761 Pérez-Donoso, A. G., Lenhof, J. J., Pinney, K., & Labavitch, J. M. (2016). Vessel embolism
762 and tyloses in early stages of Pierce's disease. *Australian Journal of Grape and Wine Research*,
763 *22*(1), 81-86. https://doi.org/10.1111/ajgw.12178

764 Pita, P., Rodríguez-Calcerrada, J., Medel, D., & Gil, L. (2018). Further insights into the
765 components of resistance to *Ophiostoma novo-ulmi* in *Ulmus minor* : Hydraulic conductance,
766 stomatal sensitivity and bark dehydration. *Tree Physiology*, *38*(2), 252-262.
767 https://doi.org/10.1093/treephys/tpx123

768 Pouzoulet, J., Mailhac, N., Couderc, C., Besson, X., Daydé, J., Lummerzheim, M., & Jacques,
769 A. (2013). A method to detect and quantify Phaeomoniella chlamydospora and
770 Phaeoacremonium aleophilum DNA in grapevine-wood samples. *Applied Microbiology and*
771 *Biotechnology*, *97*(23), 10163-10175. https://doi.org/10.1007/s00253-013-5299-6

772 Pouzoulet, J., Scudiero, E., Schiavon, M., & Rolshausen, P. E. (2017). Xylem Vessel Diameter
773 Affects the Compartmentalization of the Vascular Pathogen Phaeomoniella chlamydospora in
774 Grapevine. *Frontiers in Plant Science*, *8*, 1-13. https://doi.org/10.3389/fpls.2017.01442

775 Pouzoulet, J., Scudiero, E., Schiavon, M., Santiago, L. S., & Rolshausen, P. E. (2019).
776 Modeling of xylem vessel occlusion in grapevine. *Tree Physiology*, *39*(8), 1438-1445.
777 https://doi.org/10.1093/treephys/tpz036

778 Pouzoulet, J., Rolshausen, P. E., Charbois, R., Chen, J., Guillaumie, S., Ollat, N., Gambetta,
779 G. A., & Delmas, C. E. L. (2020). Behind the Curtain of the Compartmentalization Process :
780 Exploring How Xylem Vessel Diameter Impacts Vascular Pathogen Resistance. *Plant, Cell &*
781 *Environment*. https://doi.org/10.1111/pce.13848

782 Pratt, R. B., & Jacobsen, A. L. (2018). Identifying which conduits are moving water in woody
783 plants : A new HRCT-based method. *Tree Physiology*, *38*(8), 1200-1212.
784 https://doi.org/10.1093/treephys/tpy034

785 Rioux, D., Blais, M., Nadeau-Thibodeau, N., Lagacé, M., DesRochers, P., Klimaszewska, K.,
786 & Bernier, L. (2018). First Extensive Microscopic Study of Butternut Defense Mechanisms
787 Following Inoculation with the Canker Pathogen *Ophiognomonia clavigignenti-*
788 *juglandacearum* Reveals Compartmentalization of Tissue Damage. *Phytopathology*, *108*(11),
789 1237-1252. https://doi.org/10.1094/PHYTO-03-18-0076-R

790 Salle, A., Ye, H., Yart, A., & Lieutier, F. (2008). Seasonal water stress and the resistance of
791 *Pinus yunnanensis* to a bark-beetle-associated fungus. *Tree Physiology*, *28*(5), 679-687.
792 https://doi.org/10.1093/treephys/28.5.679

793 Salleo, S., Nardini, A., Lo Gullo, M. A., & Ghirardelli, L. A. (2002). Changes in stem and leaf
794 hydraulics preceding leaf shedding in *Castanea sativa* L. *Biologia plantarum*, *45*(2), 227-234.
795 https://doi.org/10.1023/A:1015192522354

796 Schneider, C. A., Rasband, W. S., & Eliceiri, K. W. (2012). NIH Image to ImageJ : 25 years of
797 image analysis. *Nature Methods*, *9*(7), 671-675. https://doi.org/10.1038/nmeth.2089

798 Sperry, J. S., Donnelly, J. R., & Tyree, M. T. (1988). A method for measuring hydraulic
799 conductivity and embolism in xylem. *Plant, Cell and Environment*, *11*(1), 35-40.
800 https://doi.org/10.1111/j.1365-3040.1988.tb01774.x

801 Solla, A., & Gil, L. (2002). Xylem vessel diameter as a factor in resistance of Ulmus minor to
802 Ophiostoma novo-ulmi. *Forest Pathology*, *32*(2), 123-134. https://doi.org/10.1046/j.1439-
803 0329.2002.00274.x

804 Sun, Q., Rost, T. L., & Matthews, M. A. (2008). Wound-induced vascular occlusions in *Vitis*
805 *vinifera* (Vitaceae) : Tyloses in summer and gels in winter. *American Journal of Botany*,
806 *95*(12), 1498-1505. https://doi.org/10.3732/ajb.0800061

807 Sun, Q., Sun, Y., Walker, M. A., & Labavitch, J. M. (2013). Vascular Occlusions in Grapevines
808 with Pierce's Disease Make Disease Symptom Development Worse. *Plant Physiology*, *161*(3),
809 1529-1541. https://doi.org/10.1104/pp.112.208157

810 Surico, G., Marchi, G., Ferrandino, A., Braccini, P., & Mugnai, L. (2000). Analysis of the
811 spatial spread of esca in some Tuscan vineyards (Italy). *Phytopathologia Mediterranea*, *39*,
812 211-224.

813 Talboys, P. W. (1972). Resistance to Vascular Wilt Fungi. *Proceedings of the Royal Society of*
814 *London. Series B, Biological Sciences*, *181*(1064,), 319-332.

815 Torres-Ruiz, J. M., Sperry, J. S., & Fernández, J. E. (2012). Improving xylem hydraulic
816 conductivity measurements by correcting the error caused by passive water uptake. *Physiologia*
817 *Plantarum*, *146*(2), 129-135. https://doi.org/10.1111/j.1399-3054.2012.01619.x

818 Tyree, M T, & Sperry, J. S. (1989). Vulnerability of Xylem to Cavitation and Embolism. *Annu.*
819 *Rev. Plant. Physiol. Plant. Mol. Biol.*, 20.

820 Tyree, Melvin T., & Ewers, F. W. (1991). The hydraulic architecture of trees and other woody
821 plants. *New Phytologist*, *119*(3), 345-360. https://doi.org/10.1111/j.1469-8137.1991.tb00035.x

822 Úrbez-Torres, J. R., Peduto, F., Vossen, P. M., Krueger, W. H., & Gubler, W. D. (2013). Olive
823 Twig and Branch Dieback : Etiology, Incidence, and Distribution in California. *Plant Disease*,
824 *97*(2), 231-244. https://doi.org/10.1094/PDIS-04-12-0390-RE

825 Venturas, M., López, R., Martín, J. A., Gascó, A., & Gil, L. (2014). Heritability of *Ulmus minor*
826 resistance to Dutch elm disease and its relationship to vessel size, but not to xylem vulnerability
827 to drought. *Plant Pathology*, *63*(3), 500-509. https://doi.org/10.1111/ppa.12115

828 Yadeta, K. A., & J. Thomma, B. P. H. (2013). The xylem as battleground for plant hosts and
829 vascular wilt pathogens. *Frontiers in Plant Science*, *4*. https://doi.org/10.3389/fpls.2013.00097

830 Yazaki, K., Takanashi, T., Kanzaki, N., Komatsu, M., Levia, D. F., Kabeya, D., Tobita, H.,
831 Kitao, M., & Ishida, A. (2018). Pine wilt disease causes cavitation around the resin canals and
832 irrecoverable xylem conduit dysfunction. *Journal of Experimental Botany*, *69*(3), 589-602.
833 https://doi.org/10.1093/jxb/erx417

834 Zimmermann, M. H. (1979). The Discovery of Tylose Formation by a Viennese lady in 1845.
835 *IAWA Bulletin*, *2*, 51-56.

SUPPORTING INFORMATION

The following Supporting Information is available for this article:

Method S1: Image analysis of microCT scans.

Method S2. Specific stem hydraulic conductivity (k_s) measurements.

Fig. S1 (a-d). Two-dimensional reconstruction of longitudinal cross sections from X-ray microCT volumes of grapevine stems.

Fig. S2. Relationship between k_s and k_{th} in control plants.

Fig. S3. Vessel density and percentage of occluded vessels in tiger-stripe stems for different vessel diameter classes.

Fig. S4. Relationships between k_s and k_{th} in each stem symptom category.

Table S1. Effect of year of uprooting, internode analyzed, and sampling date on k_s and k_{th} in control stems.

Table S2. Calculated theoretical hydraulic conductivity (k_{th} %), and hydraulic conductivity loss (PLC %) from X-ray microCT volumes of intact grapevine stems.

FIGURES

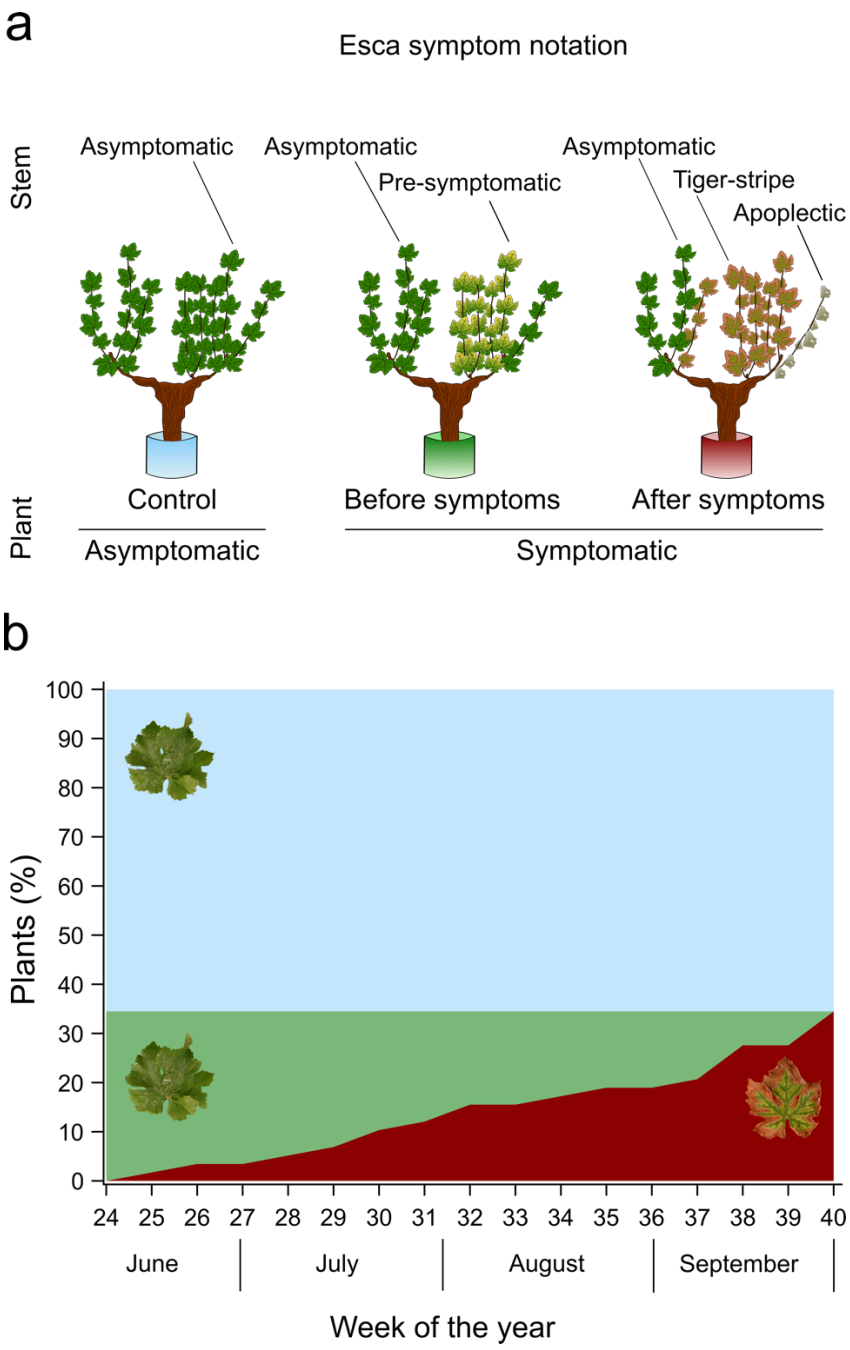

Fig. 1 (a-b). Representation of esca symptom notation during the experimental season. (**a**) Single stems could be noted as esca asymptomatic, pre-symptomatic, tiger-stripe, or apoplectic. Whole plants have been noted as control (asymptomatic from June to October) or symptomatic (with tiger-stripe symptoms at the end of the season). (**b**) Proportion of plants in each symptom category over the experimental season (n=58). The blue area corresponds to control plants, green area to esca symptomatic plants before symptom appearance, and red area to esca symptomatic plants.

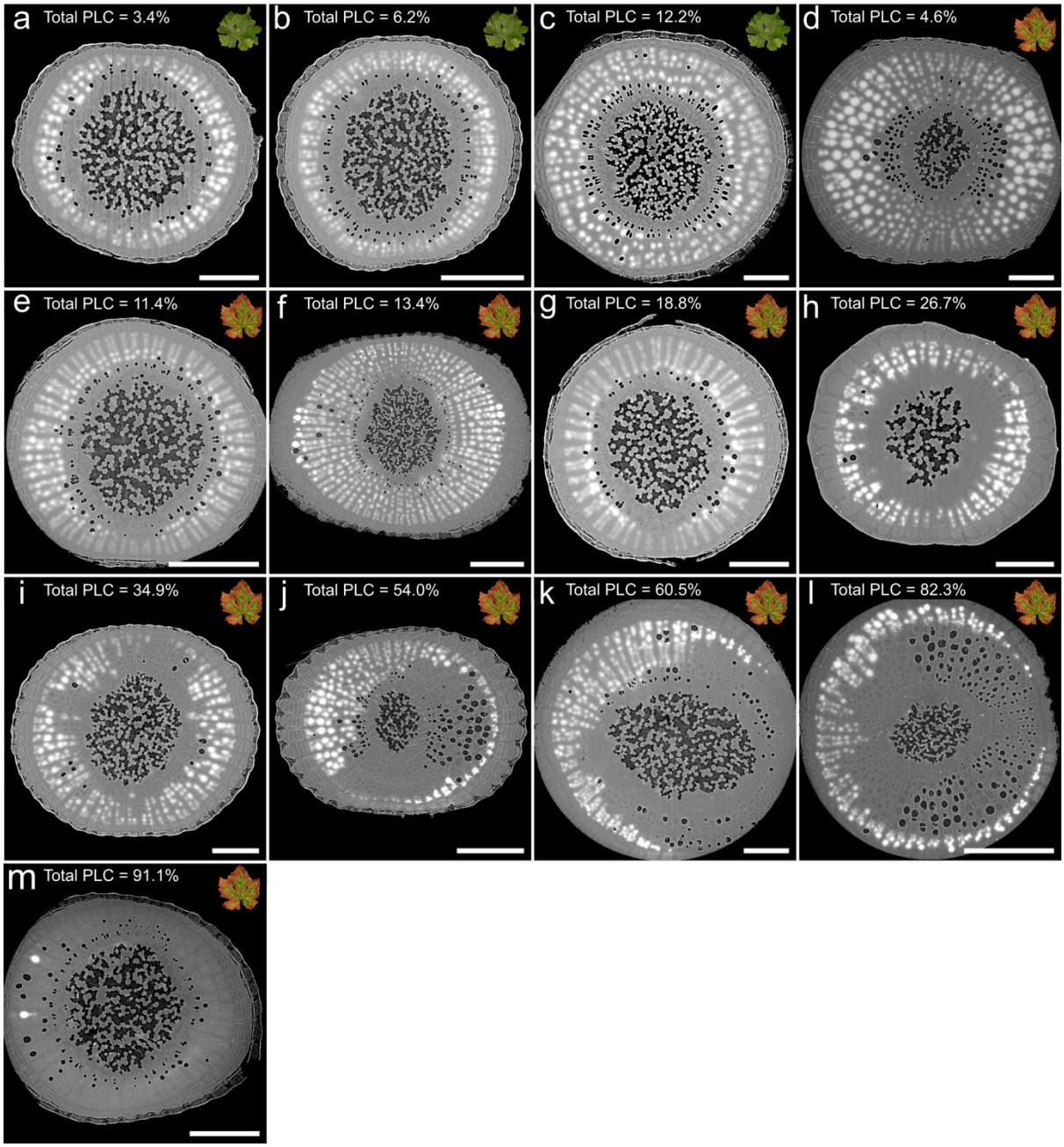

Fig. 2 (a-m). Two-dimensional reconstruction of cross-sections from X-ray microCT volumes of grapevine stems. Each panel represents a cross section of different stems for control (**a-c**) and esca symptomatic (**d-m**) plants. Iohexol appears white bright in functional vessels; air-filled vessels (i.e. native PLC) appear black; occluded vessels (i.e. occlusion PLC) appear grey. Total PLC (i.e. native PLC plus occlusion PLC) values are given for the presented samples. Scale bars = 1000µm.

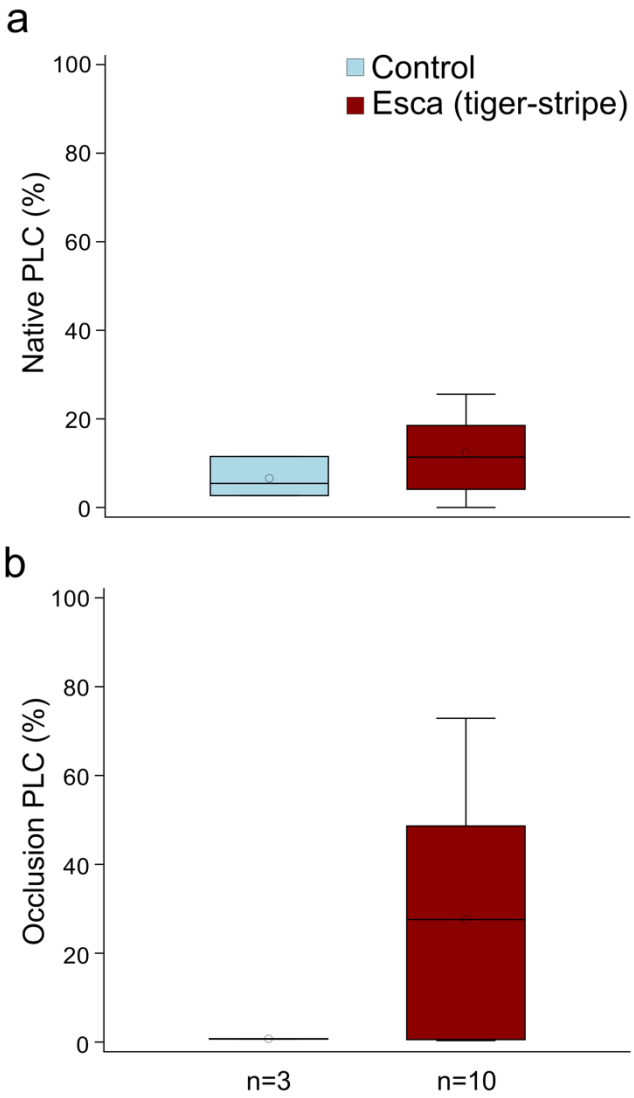

Fig. 3 (a-b). **(a)** Mean values of native PLC in control (blue) and esca tiger-stripe (red) stems of grapevine plants using X-ray microCT imaging. Differences were not significant (n=13, $F_{1,9}$=0.07, P=0.79). **(b)** Mean values of occlusion PLC in control (blue) and esca tiger-stripe (red) stems of grapevine plants using X-ray microCT imaging. Differences were not significant (n=13, $F_{1,9}$=0.33, P=0.58). Boxes and bars show the median, quartiles and extreme values, circles show mean values. N represents the sample size (number of analyzed stems) for each group.

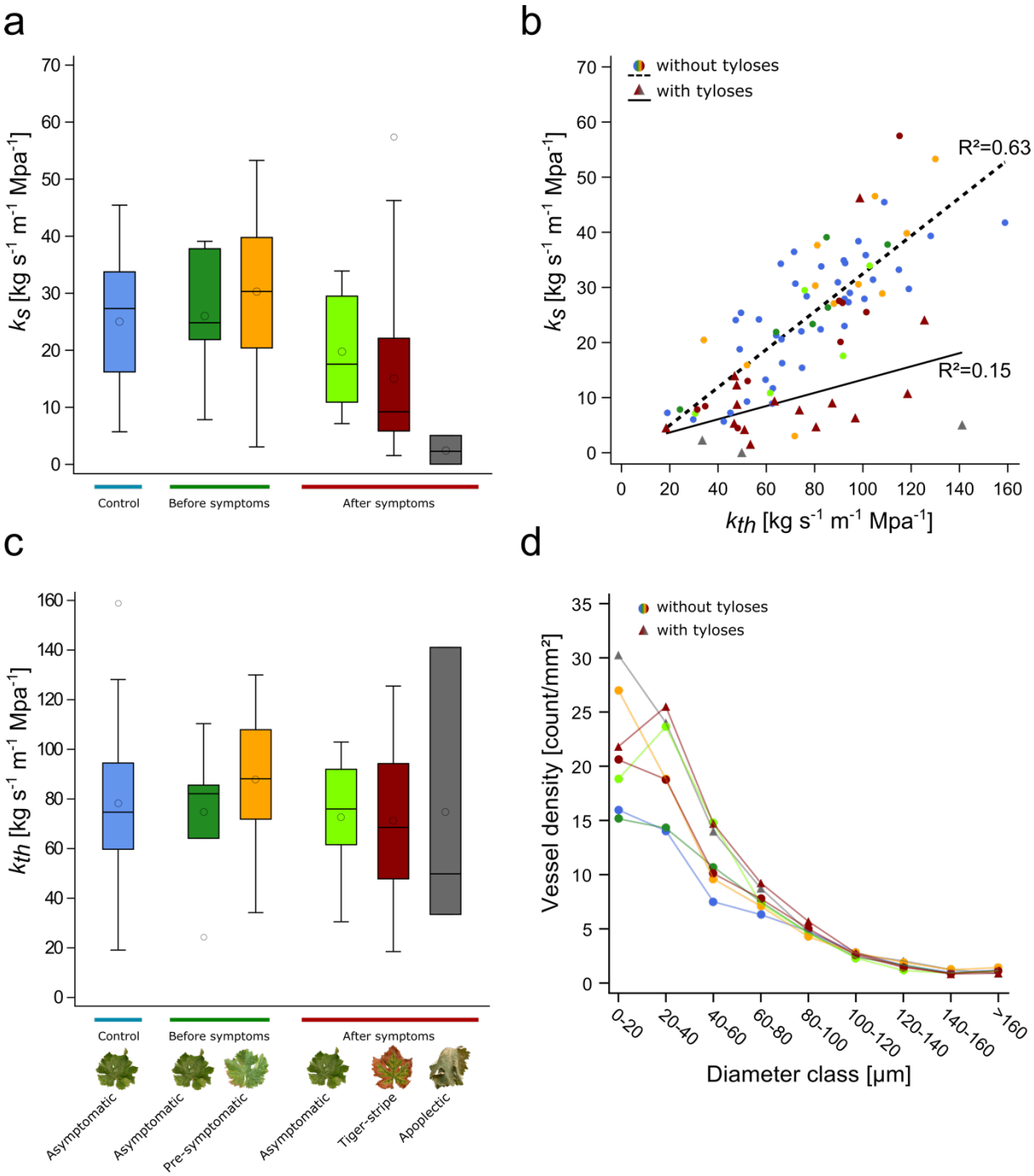

Fig. 4 (a-d). Relationships between specific stem hydraulic conductivity (k_s), theoretical stem hydraulic conductivity (k_{th}), and vessel density in control and esca symptomatic grapevine plants. **(a)** k_s values for control (blue); asymptomatic (dark green) and pre-symptomatic (yellow) stems in plants before symptom appearance; asymptomatic (light green), tiger-stripe (red), and apoplectic (grey) stems in plants after symptom appearance, differences were not significant (n=88, $F_{5,45}$=1.30 P=0.28). Boxes and bars show the median, quartiles and extreme values, circles within boxes correspond to means, and circles outside boxes to outlier values. **(b)** Relationships between k_s and k_{th}. Symbols represent the absence (circles) or presence

(triangles) of tyloses in xylem vessels. Colors represent esca symptomatology (as in panel a). The dashed line represents the regression for stems in which no tyloses were observed in xylem vessels, and the solid line represents the regression for samples with tyloses. R^2 for the regression lines are indicated (see Table 2 and Fig. S4 for detailed analyses). **(c)** k_{th} values for the different stem categories as presented in panel a. Differences were not significant (n=88, $F_{5,45}$=0.58, P=0.71). **(d)** Relationships between mean values of xylem vessel density and their diameters. Differences in total vessel density and in vessel size distributions were not significant (n=88, $F_{6,45}$=0.77, P=0.60; n=792 (88 samples for 9 vessel classes), $F_{48,693}$=1.19, P=0.18). Colors and markers are the same as panel b.

TABLES

Table 1. Esca leaf symptom observations over the experimental season on *Vitis vinifera* cv Sauvignon blanc.

Symptom notation before 2019 / **Symptom notation in 2019**	**All plants**	**Previously asymptomatic (pA)**	**Previously symptomatic (pS)**
Esca-symptomatic	35 % (20/58)	30 % (6/20)	37 % (14/38)
Control-asymptomatic	65 % (38/58)	70 % (14/20)	63 % (24/38)

Plants are grouped by their symptom history: previously asymptomatic (pA, plants that have never expressed leaf symptoms between 2012 and 2018) and previously symptomatic (pS, plants that have expressed leaf symptoms at least once since 2012). Ratios present the number of plants in each symptom category (esca-symptomatic or control-asymptomatic) over the total number of plants of the category.

Table 2. Values for specific stem hydraulic conductivity (k_s), theoretical stem hydraulic conductivity (k_{th}) and equations of regression lines between k_s and k_{th} for control and esca symptomatic stems.

Tyloses	Esca	k_s [kg s^{-1} m^{-1} Mpa^{-1}]	k_{th} [kg s^{-1} m^{-1} Mpa^{-1}]	n (stem - plant)	Regression
Absence	Control	24.97 ± 1.72	78.36 ± 4.51	39 - 23	k_s = 0.3 x k_{th} + 1.6 R^2=0.61 P<0.0001
	Asymptomatic before symptoms	26.04 ± 4.71	74.75 ± 11.80	6 - 6	k_s = 0.36 x k_{th} - 0.94 R^2=0.82 P=0.013
	Pre-symptomatic	30.32 ± 4.26	87.88 ± 8.54	11 - 7	k_s = 0.37 x k_{th} - 1.9 R^2=0.54 P=0.010
	Asymptomatic after symptoms	19.80 ± 5.18	72.58 ± 12.64	5 - 2	k_s = 0.33 x k_{th} - 4 R^2=0.64 P=0.104
	Esca (tiger-stripe)	21.29 ± 5.40	72.85 ± 10.41	9 - 5	k_s = 0.45 x k_{th} - 11.26 R^2=0.74 P=0.003
Presence	Esca (tiger-stripe)	11.27 ± 2.86	70.44 ± 7.81	15 - 5	k_s = 0.17 x k_{th} -0.84 R^2=0.22 P=0.077
	Esca (apoplectic)	2.47 ± 1.45	74.80 ± 33.48	3 - 2	k_s = 0.04 x k_{th} - 0.2 R^2=0.68 P=0.385
Absence	All	25.06 ± 1.46	78.42 ± 3.37	70 - 37	k_s = 0.34 x k_{th} - 1.90 R^2=0.63 P<0.0001
Presence	All	9.81 ± 2.51	71.16 ± 8.00	18 - 7	k_s = 0.12 x k_{th} - 1.28 R^2=0.15 P=0.117

Values represent mean ± SE. n = sample size, (including the number of analyzed stems and-number of analyzed plants, respectively). See text and Fig. 4 for statistical analysis. A detailed esca symptom notation is provided in Fig. 1a. Bivariate plots of each regression are presented in Fig. S4.

910 **Table 3**. Long-term impact of symptom presence (i.e. comparing plants with different disease
911 history record) in control plants on specific stem hydraulic conductivity (k_s), theoretical stem
912 hydraulic conductivity (k_{th}), stem total vessel density, and amount of *Phaeomoniella*
913 *chlamydospora* and *Phaeoacremonium minimum* DNA in trunks.
914

	Previously asymptomatic (pA)	**Previously asymptomatic (pS)**	**Type III Tests of Fixed Effects (pA vs pS)**
k_s [kg s^{-1} m^{-1} Mpa^{-1}]	23.76 ± 2.30	26.54 ± 2.61	n=39, $F_{1,16}$=1.19, P=0.29
k_{th} [kg s^{-1} m^{-1} Mpa^{-1}]	72.22 ± 4.85	86.30 ± 7.98	n=39, $F_{1,16}$=3.01, P=0.10
total vessel density [count mm^{-2}]	57.28 ± 4.03	52.61 ± 3.25	n=39, $F_{1,16}$=0.72, P=0.41
P. chlamydospora [pg ng^{-1}]	6.14 ± 1.90	10.15 ± 3.41	**n=13, $F_{1,11}$=5900.06, P<0.0001**
P. minimum [pg ng^{-1}]	9.27 ± 6.97	26.40 ± 13.83	**n=13, $F_{1,11}$=51014, P<0.0001**

915 Values represent means ± SE. Pathogen quantification was estimated as: pg fungal DNA ng^{-1}
916 total DNA. Statistical tests used are individual generalized linear mixed models to compare pA
917 vs pS plants (fixed effect) with the individual plants entered as a random effect in the models
918 and the year of uprooting as a co-variable (fixed effect). Statistically significant results
919 (P<0.05) are shown in bold.

Table 4. Quantification by qPCR of *Phaeomoniella chlamydospora* and *Phaeoacremonium minimum* DNA in stems and trunks of different esca symptomatology.

Organ	Esca	n	*P. chlamydospora* [pg ng^{-1}]	*P. minimum* [pg ng^{-1}]
Stem	Control	8	0	0
	Pre-symptomatic	3	0	0
	Asymptomatic (after symptoms)	3	0	0
	Tiger-stripe (without tyloses)	4	0	0
	Tiger-stripe (with tyloses)	8	0	0
	Apoplectic	2	0	0
Trunk	Control	13	7.37 ± 1.67 (12/13)*	14.54 ± 6.51 (12/13)*
	Symptomatic	7	15.80 ± 3.12 (7/7)*	23.90 ± 8.82 (7/7)*

* Number of samples positive for the pathogen over the total number of analyzed samples.

Pathogen quantification was estimated as: pg fungal DNA per ng total DNA.Values represent means ± SE, n = sample size. Trunks of symptomatic plants presented higher amount of both *P. chlamydospora* and *P. minimum*, compared to control (n=20, $F_{1,18}$=29806.11.25, P<0.0001 and n=20, $F_{1,18}$=21925.4, P<0.0001, respectively). See text for statistical methods.